Proceedings of the 54th Israel Annual Conference
on Aerospace Sciences, Tel-Aviv & Haifa, Israel,
February 19-20, 2014

Transition to turbulence in Couette flow

M. Karp and J. Cohen
Faculty of Aerospace engineering, Technion - Israel Institute of Technology,
Haifa 32000, Israel

This paper describes a study of transition in Couette flow initiated by the transient growth mechanism. It is shown that four modes obtained analytically are sufficient to model the transient growth. The analytical approximation allows performing a secondary stability analysis of the modified baseflow consisting of the Couette flow and a transient growth perturbation. The predictions of the secondary stability analysis are verified by checking whether transition occurs in a direct numerical simulation (DNS) initiated by the analytical expressions. Finally, the capability of the analytical expressions to capture some of the transition stages is tested.

I. Introduction

Despite much progress in the field of fluid mechanics over the last century, prediction of transition to turbulence - namely, the critical Reynolds number separating the laminar and turbulent regimes, remains a puzzling issue. At first, linear stability theory (LST) has been used to calculate the critical Reynolds number for given flow conditions. However, for some basic flows, such as plane Couette flow, the LST has not been successful in predicting the critical Reynolds since the flow is linearly stable (e.g. [1]), whereas transition has been observed in experiments at Reynolds numbers greater than $Re \sim 360$. A possible explanation for such transition phenomenon has been proposed by the mechanism of non-modal growth where a disturbance can grow linearly with time in an inviscid base flow [2]. Such a disturbance is a three-dimensional one which is invariant along the streamwise direction. For viscous base flows, it has been shown [3] that a disturbance can achieve initial significant growth before its eventual exponential decay due to viscous effects. This mechanism is called transient growth. Thus, a possible explanation for transition in linearly stable flows could be that a small disturbance is amplified significantly by transient growth such that nonlinear effects are triggered and transition occurs rapidly, before the disturbance decays. Much research has been carried out to find the initial optimal disturbances which yield the maximal growth over a given time or distance. It has been shown that the maximal growth is obtained by a disturbance initially consisting of a pair nearly streamwise independent counter-rotating vortices. These vortices create streamwise streaks which vary along the spanwise direction (with a wavenumber β) by lifting low momentum fluid into a region of high momentum fluid and vise versa. The counter-rotating vortices mainly consist of a pair of nearly parallel least stable modes, as demonstrated by [4] and [5]. Numerical simulations have shown that these streaks may undergo secondary instability [6] and can lead to transition to turbulence (e.g. [7] for pipe flow).

In this paper we show that linear transient growth can be modeled using only four modes which are obtained analytically. The analytical approximation allows performing a secondary stability analysis of the perturbed baseflow consisting of the Couette flow

and a transient growth disturbance. The predictions of the secondary stability analysis are verified by checking whether transition occurs in a DNS initiated by the analytical expressions. Finally, the ability of the analytical expressions to follow the transition stages is discussed.

II. Mathematical Method

The linear transient growth is traditionally estimated from the gain, $G(t)$, of the disturbance kinetic energy, $E(t)$, at time t normalized by its initial value, $E(t=0)$, where the energy is defined by the volumetric integral over the whole domain, i.e.,

$$G(t) = \frac{E(t)}{E(t=0)}; \qquad E(t) = \frac{1}{4L_xL_z}\int_0^{L_z}\int_{-1}^{1}\int_0^{L_x}(u^2+v^2+w^2)dxdydz. \tag{1}$$

Here, $\boldsymbol{x} = (x, y, z)$ is the position vector for which x, y and z are the streamwise, wall-normal and spanwise coordinates, respectively, and u, v and w are the corresponding velocity components. A pair of nearly parallel least stable modes is sufficient to understand the physical mechanism of transient growth, but does not predict the growth of the disturbance [4]. However, as we show, the addition of a second pair of modes allows obtaining a good analytical approximation to transient growth (i.e, the approximation is based on four modes). The modes are obtained by solving the well known Orr-Sommerfeld (OS) equation for the vertical velocity (v) and the Squire (Sq) equation for the vertical vorticity ($\eta = \frac{\partial u}{\partial z}$) for the case of streamwise independent perturbations:

$$\left\{\frac{\partial}{\partial t} - \frac{1}{Re}\boldsymbol{\nabla}^2\right\}\boldsymbol{\nabla}^2 v = 0, \tag{2a}$$

$$\left\{\frac{\partial}{\partial t} - \frac{1}{Re}\boldsymbol{\nabla}^2\right\}\eta = \Omega\frac{\partial v}{\partial z}, \tag{2b}$$

where $\Omega = -\frac{dU_0}{dy}$ is the baseflow vorticity. The boundary conditions are:

$$\eta(y=\pm1) = 0;\ v(y=\pm1) = 0;\ \mathcal{D}v(y=\pm1) = 0, \tag{3}$$

where $\mathcal{D} \equiv \frac{\partial}{\partial y}$. It is assumed the disturbance has the spanwise wavenumber β and the temporal eigenvalue ω:

$$\boldsymbol{q} = \tilde{\boldsymbol{q}}(y)e^{i\beta z - i\omega t}, \tag{4}$$

where $\boldsymbol{q} = (u; v; w; p)$. The solution of the above equation yields many modes, including even (symmetric) modes as well as odd (antisymmetric) ones. We proceed by taking only four (least stable) modes as an approximation to the transient growth disturbance. Consequently, the disturbance has the following form:

$$\boldsymbol{u}_1(t, y, z) = \Re\left\{\sum_{m=1}^{4} A_m \boldsymbol{u}_m(y)e^{i\beta z - i\omega_m t}\right\}. \tag{5}$$

The ratios between the four modes, i.e. the coefficients A_m, are found by letting $A_4 = 1$ and optimize the remaining three coefficients to maximize the energy growth. It should be noted that the coefficients are obtained analytically. The optimal even disturbance (based on four even modes) corresponds to a single Counter-rotating Vortex Pair (CVP)

centered at the middle of the channel, whereas the optimal odd disturbance (based on four odd modes) corresponds to two CVPs, placed symmetrically in the top and bottom parts of the channel. These patterns of the initial even and odd optimal disturbances agree well with previously obtained numerical results based on numerous modes (e.g. [8]).

During the validation of our four mode approximation with DNS (not shown here) we discovered that nonlinear interactions play an important role in the stability of the modified baseflow (Couette plus transient growth perturbation). Therefore, an asymptotic expansion has been performed to find the nonlinear modification of the transient growth. Accordingly, the velocity field has been written by ($A_0 \ll 1$),

$$\boldsymbol{u} = \boldsymbol{U}_0(y) + A_0\boldsymbol{u}_1(t,y,z) + A_0^2\boldsymbol{u}_2(t,y,z) + \cdots \tag{6}$$

where $\boldsymbol{U}_0(y) = (0, y, 0)$ is the Couette flow, $A_0\boldsymbol{u}_1$ describes the transient growth perturbation (four modes) and $A_0^2\boldsymbol{u}_2$ its nonlinear modification. The latter has been calculated by substituting eq. (6) into the incompressible Navier-Stokes equations and writing the equations at order $O(A_0^2)$. This leads to the following equations for v_2 and $\eta_2 = \frac{\partial u_2}{\partial z}$:

$$\left\{\frac{\partial}{\partial t} - \frac{1}{Re}\boldsymbol{\nabla}^2\right\}\boldsymbol{\nabla}^2 v_2 = -\frac{\partial}{\partial z}\left\{\frac{\partial R_b}{\partial z} - \frac{\partial R_c}{\partial y}\right\}, \tag{7a}$$

$$\left\{\frac{\partial}{\partial t} - \frac{1}{Re}\boldsymbol{\nabla}^2\right\}\eta_2 = \Omega\frac{\partial v_2}{\partial z} - \frac{\partial R_a}{\partial z}, \tag{7b}$$

subjected to the following boundary and initial conditions:

$$\eta_2(t=0) = 0; \eta_2(y=\pm 1) = 0; v_2(t=0) = 0; v_2(y=\pm 1) = 0; \mathcal{D}v_2(y=\pm 1) = 0, \tag{8}$$

where $\mathcal{D} \equiv \frac{\partial}{\partial y}$. The right hand side expressions are given by interactions among the four modes constituting the transient growth ($\boldsymbol{u}_1$):

$$R_a = v_1\frac{\partial u_1}{\partial y} + w_1\frac{\partial u_1}{\partial z}, \tag{9a}$$

$$R_b = v_1\frac{\partial v_1}{\partial y} + w_1\frac{\partial v_1}{\partial z}, \tag{9b}$$

$$R_c = v_1\frac{\partial w_1}{\partial y} + w_1\frac{\partial w_1}{\partial z}. \tag{9c}$$

These equations have been solved using Duhamel's principle.

The analytical expressions for the velocity field allow performing a secondary stability analysis of the modified baseflow. As the modified baseflow depends on both wall-normal and spanwise directions, a two dimensional linear stability analysis is necessary (e.g. [9]). The analysis is conducted using the Floquet theory since the baseflow is periodic in the spanwise direction with the wavelength $2\pi/\beta$. A necessary assumption for performing the stability analysis is that the time scale of the streak transient growth and decay is much smaller than the time scale associated with the growth of the secondary instability. This allows separation of time scales and performing the stability analysis for a particular 'frozen' time. Another assumption is that relative to the streamwise velocity, the wall-normal and spanwise velocities of the base flow are negligible. We assume a secondary disturbance of the form:

$$\boldsymbol{q} = e^{i(\alpha x - \omega t)}\sum_{k=-M_z}^{M_z}\hat{\boldsymbol{q}}_k(y)e^{i\beta k z} \tag{10}$$

where $\boldsymbol{q} = (u; v; w; p)$, α is the streamwise wavenumber and ω is the temporal complex eigenvalue. Substituting the disturbance in the linearized Navier-Stokes equations allows obtaining an eigenvalue problem for the calculation of the eigenvalues ω_n and the eigenfunctions $(u_n; v_n; w_n; p_n)$, where the subscript n indicates the n-th eigenvalue for given Re, α, β and t_s (the 'frozen' time for the stability analysis). The use of an analytical expression for the base flow allows convergence for relatively small values of M_z and it is found that $M_z = 5$ is sufficient to obtain the eigenvalues within accuracy of 0.5%. The eigenvalue problem is solved numerically using MATLAB with 101 Chebyshev modes in the wall-normal direction.

The predictions of the secondary stability analysis are verified by checking whether transition occurs when simulating the secondary disturbance in the modified baseflow. The DNS is initiated by the analytical expressions, with most of the initial energy in the transient growth perturbation and a very small fraction of energy in the secondary disturbance. The simulation used in this study is Gibson's well-tested 'Channelflow' DNS software [10]. The simulation code is pseudospectral, using Fourier modes in the x and z directions and Chebyshev (Collocation) modes in the y direction with no-slip and impermeability on the walls at $y = \pm 1$. The computational box contains five wavelengths in the streamwise direction and a single wavelength in the spanwise direction $L_x = 10\pi/\alpha, L_z = 2\pi/\beta$. The results are obtained on a grid containing $(256, 65, 64)$ points in the x, y and z directions, respectively. It is found that increasing the number of modes improves the accuracy, however, its influence on the disturbance energy is minor. In order to remove aliasing the 3/2 rule is applied so that the number of corresponding Fourier modes is $N'_{x,z} = \frac{2}{3}N_{x,z}$. The time step is chosen to obtain an initial Courant-Friedrichs-Lewy (CFL) number of 0.17.

To summarize this section, our velocity field consists of four analytically obtained elements:

$$\boldsymbol{u} = \boldsymbol{U}_0(y) + A_0\boldsymbol{u}_1(t, y, z) + A_0^2\boldsymbol{u}_2(t, y, z) + A_d\boldsymbol{u}_d(t, x, y, z) \tag{11}$$

where $\boldsymbol{U}_0(y) = (0, y, 0)$ is the Couette flow, $A_0\boldsymbol{u}_1$ describes the transient growth perturbation (four modes), $A_0^2\boldsymbol{u}_2$ its nonlinear modification and $A_d\boldsymbol{u}_d(t, x, y, z)$ the secondary disturbance obtained from the stability analysis.

III. Results

The energy growth of the optimal odd transient growth disturbance at Reynolds number of $Re = 1000$ and a spanwise wavenumber $\beta = 1$ is shown by the black solid line in figure 1. The corresponding analytical curve based on four modes is shown by the dashed red line. It can be seen that the analytical approximation follows closely the optimal curve based on numerous modes.

An example of a transition scenario for the case above (odd perturbation, $Re = 1000$ and $\beta = 1$) is indicated by the blue solid line in figure 2. The initial energy (per unit volume) of the total disturbance has been set to $E_0 = 2.66 \times 10^{-4}$ (corresponding to $A_0 = 0.01$), where the energy of the secondary disturbance is $A_d = 0.09\%$ of the total disturbance energy. The secondary disturbance is based on a stability analysis which includes nonlinear interactions at $t_s = 20$ for $\alpha = 1$. The unperturbed transient growth scenario ($A_d = 0$) is presented as well by the dashed red line. Initially both curves grow together until transition occurs rapidly at $t \approx 45$.

A transition scenario for the even transient growth perturbation has been obtained is a similar manner for $Re = 1000$ and $\beta = 2$ using the same total initial energy and fraction

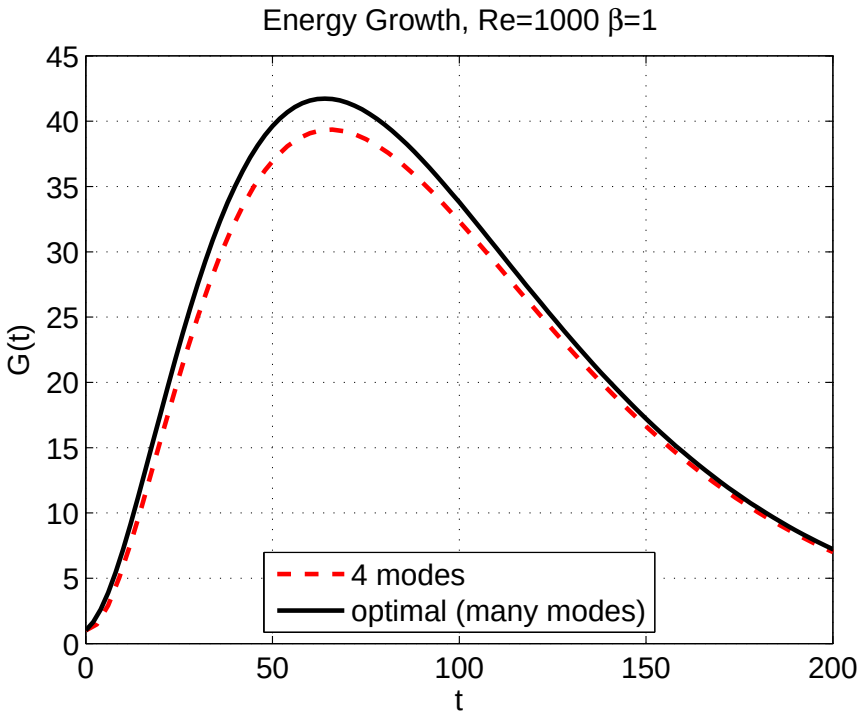

Figure 1. Energy growth curve for the odd disturbance for $Re = 1000$ and $\beta = 1$, comparison between the analytical curve based on four modes and the optimal curve based on many modes.

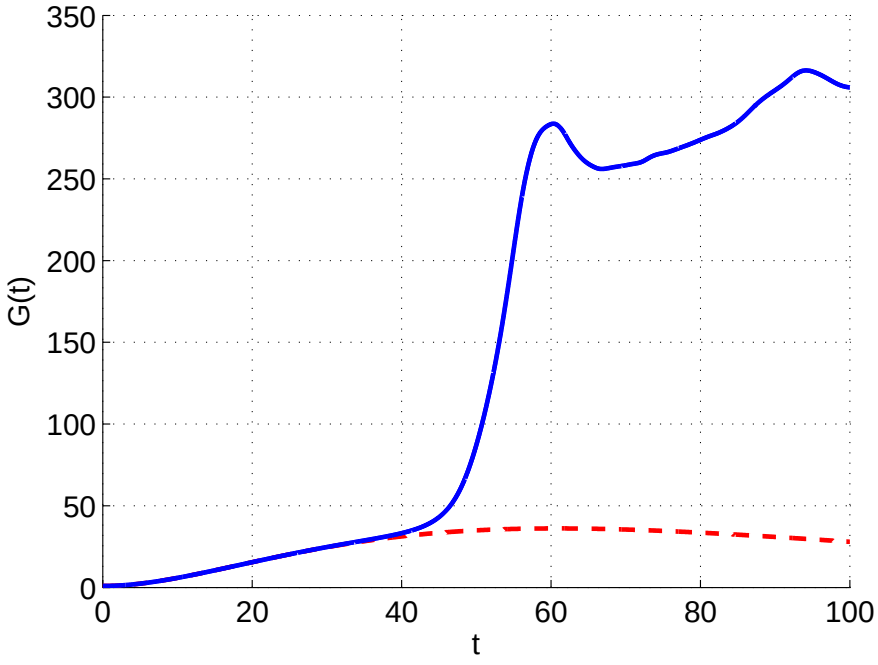

Figure 2. Energy growth obtained by DNS based on four odd modes and a secondary disturbance for $Re = 1000, \beta = 1$ and $E_0 = 2.66 \times 10^{-4}$. The secondary disturbance is based on a stability analysis which includes nonlinear interactions at $t_s = 20$ for $\alpha = 1$. The solid line corresponds to $A_d = 0.09\%$. The unperturbed transient growth ($A_d = 0$) is given for reference (dashed line).

of energy in the secondary disturbance ($E_0 = 2.66 \times 10^{-4},\ A_d = 0.09\%$). The secondary disturbance is based on a stability analysis which includes nonlinear interactions at $t_s = 20$ for $\alpha = 1$. The transition scenario is indicated by the blue solid line in figure 3 together with the unperturbed transient growth scenario ($A_d = 0$) indicated by the dashed red line. It can be seen that the transition occurs rapidly in a similar manner to the odd scenario. Comparing between the even and the odd scenarios we observe that the unperturbed even transient growth reaches a higher kinetic energy gain ($G_{max} \sim 460$ and $G_{max} \sim 40$ for the even and odd perturbations, respectively). Nevertheless, after transition occurs the gain in both cases attains similar values ($G(t) \sim 250 - 320$).

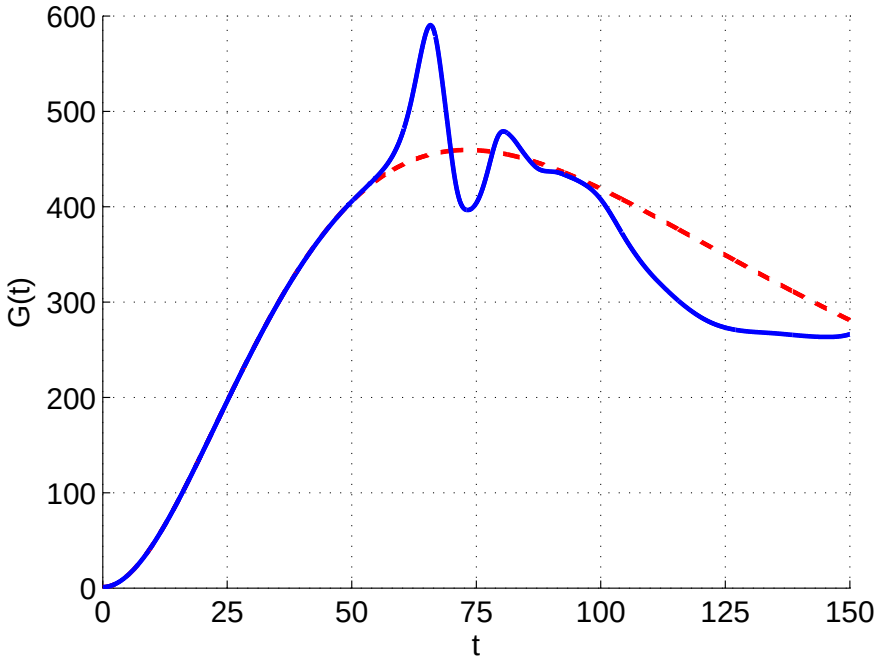

Figure 3. Energy growth obtained by DNS based on four even modes and a secondary disturbance for $Re = 1000, \beta = 2$ and $E_0 = 2.66 \times 10^{-4}$. The secondary disturbance is based on stability analysis which includes nonlinear interactions at $t_s = 20$ for $\alpha = 1$. The solid line corresponds to $A_d = 0.09\%$. The unperturbed transient growth ($A_d = 0$) is given for reference (dashed line).

The evolution of the vortical structures corresponding to the odd transition scenario shown in figure 2 is presented in figure 4. To identify the vortical structure, Q, the second invariant of the velocity gradient tensor, is used ($Q = -0.5\partial u_i/\partial x_j \cdot \partial u_j/\partial x_i$ [11]). Only half of the domain is shown since the structures evolve symmetrically with respect to the y axis (for each hairpin moving downstream in the top-half domain there is a hairpin moving in the opposite direction in the bottom-half domain). The initially streamwise CVP (figure 4a) experiences a streamwise symmetric wavy modulation, which is enhanced by $t = 15$ (figure 4b). At $t = 25$ (figure 4c) streamwise-periodical spanwise vortical segments are formed above the wavy CVP which later join with the streamwise vortical elements situated beneath them. Consequently, a packet of hairpins is formed ($t = 40$, figure 4d). The packet further intensifies and the hairpin 'heads' become more localized having a shape of loops ($t = 50$, figure 4e). Shortly afterwards (not shown here) the flow becomes turbulent.

The evolution of the vortical structures corresponding to the even transition scenario

shown in figure 3 is presented in figure 5. The initially streamwise CVP (figure 5a) experiences a streamwise antisymmetric wavy modulation, which is enhanced by $t = 20$ (figure 5b). By $t = 35$ (figure 5c) the vortices split and each element splits again by $t = 55$ figure (5d). Finally, just before transition occurs, oblique alternating vortices are formed in the lower-middle and upper-side parts of the computational domain ($t = 65$, figure 4e).

Next we try to follow analytically the above DNS vortex dynamics using the analytical expressions for $\boldsymbol{u}_1(t, y, z), \boldsymbol{u}_2(t, y, z)$ and $\boldsymbol{u}_d(t, x, y, z)$ in eq. (11). The temporal evolution of the transient growth is known. On the other hand, although the growth rate and eigenfunction of the secondary disturbance ,$\boldsymbol{u}_d(t, x, y, z)$, are known for any given time, its overall integrated temporal evolution has not been derived analytically. Nevertheless, for the purpose of this section the secondary disturbance is assumed to have a constant growth rate and a fixed eigenfunction corresponding to a specific time. Here we choose this time to be $t_s = 20$ since this is the time used to obtain the secondary disturbances that initiated the DNS.

The temporal vortical dynamics based on eq. (11) for the parameters of the odd transition (figure 4) are presented in figure 6. It can be seen that all essential stages described earlier for the DNS simulation appear here too (figures 4a,b,c,d compared with figures 6a,b,c,d, respectively), except the final stage (figure 4e) at which additional nonlinear interactions should be taken into account. The corresponding temporal vortical dynamics for the parameters of the even transition (figure 5) are presented in figure 7. As in the odd scenario, the initial stages are captured quite well here too. However, the last two stages before transition (figures 5d,e) are not captured well probably due to additional nonlinear effects which have not been derived at this stage. Because of the assumption on the temporal evolution of the secondary disturbance, the different stages are well captured but not at the right times. Nevertheless, it is clear that the physical process is obtained correctly. Choosing different t_s for obtaining the secondary disturbance eigenvalue and eigenfunction, leads to the same stages of evolution that occur at different times. It can be seen that the relatively small number of modes in the analytical approximation enables us to follow most of the process analytically.

IV. Conclusions

It is shown that four decaying modes are sufficient to approximately follow the transient growth scenario in plane Couette flow. This enables us to follow analytically the early stages of the transition scenario. This is demonstrated for two types of transient growth perturbations. Future research will include the sensitivity to various parameters such as Re and β.

Acknowledgments

This research was supported by the Israeli Science Foundation under Grant No. 1394/11. M. Karp would like to thank the Israeli Ministry of Science, Technology and Space for their travel support grant.

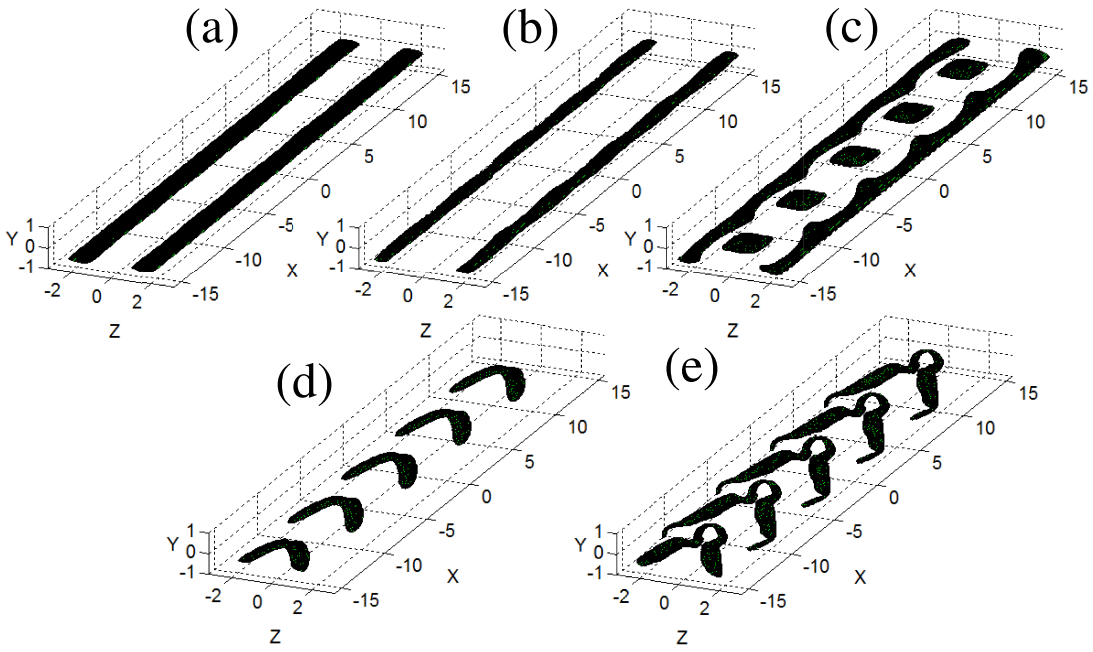

Figure 4. Vortex dynamics during transition as obtained from DNS based on an odd transient growth perturbation. Only half of the domain is shown since the structures evolve symmetrically with respect to the y axis. (a) $t = 0$, $Q/Q_{max} = 0.7$; (b) $t = 15$, $Q/Q_{max} = 0.7$; (c) $t = 25$, $Q/Q_{max} = 0.3$; (d) $t = 40$, $Q/Q_{max} = 0.3$; (e) $t = 50$, $Q/Q_{max} = 0.11$.

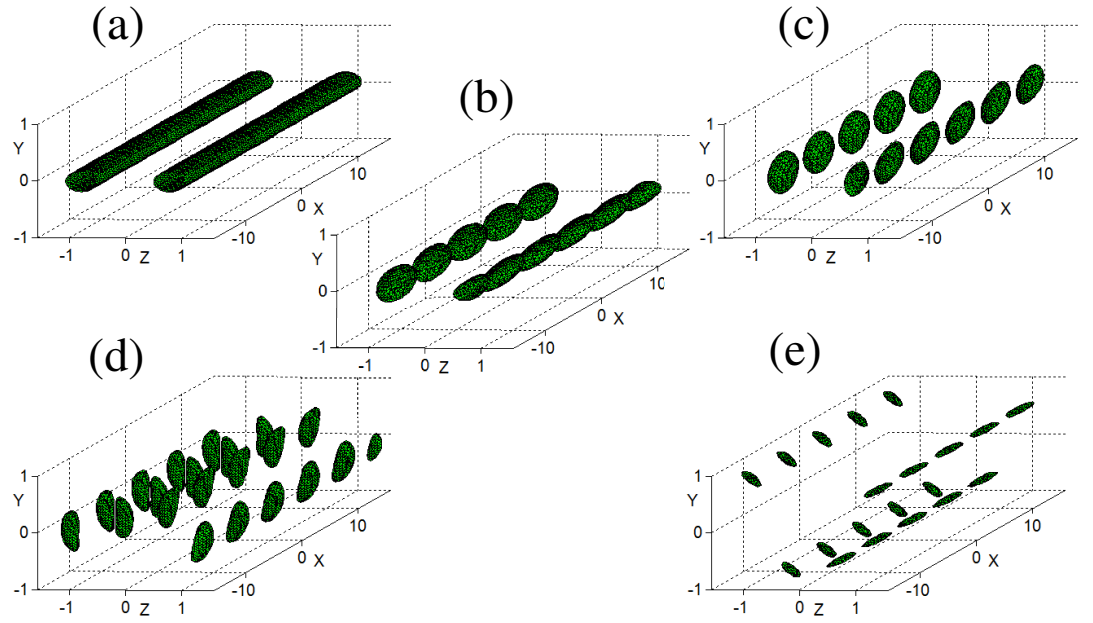

Figure 5. Vortex dynamics during transition as obtained from DNS based on an even transient growth perturbation. (a) $t = 0$, $Q/Q_{max} = 0.7$; (b) $t = 20$, $Q/Q_{max} = 0.7$; (c) $t = 35$, $Q/Q_{max} = 0.7$; (d) $t = 55$, $Q/Q_{max} = 0.7$; (e) $t = 60$, $Q/Q_{max} = 0.7$.

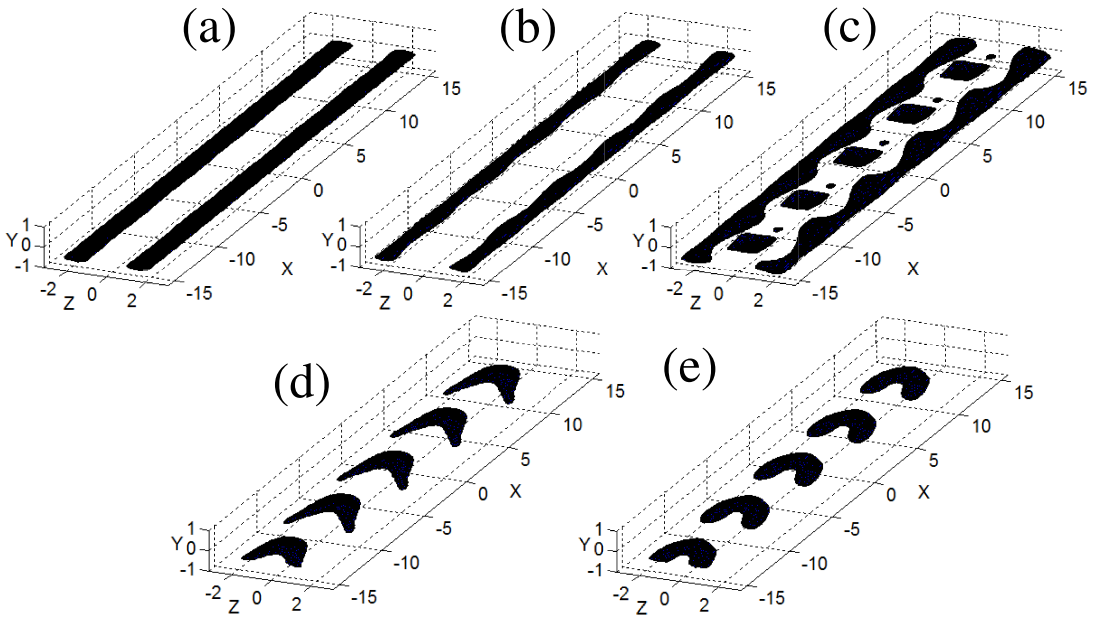

Figure 6. Vortex dynamics during transition as obtained analytically for the odd transient growth perturbation. The secondary disturbance is assumed to have a constant growth rate and eigenfunction corresponding to $t_s = 20$. The plotting method is identical to figure 4. (a) $t = 0$, $Q/Q_{max} = 0.7$; (b) $t = 10$, $Q/Q_{max} = 0.7$; (c) $t = 20$, $Q/Q_{max} = 0.3$; (d) $t = 30$, $Q/Q_{max} = 0.3$; (e) $t = 40$, $Q/Q_{max} = 0.3$.

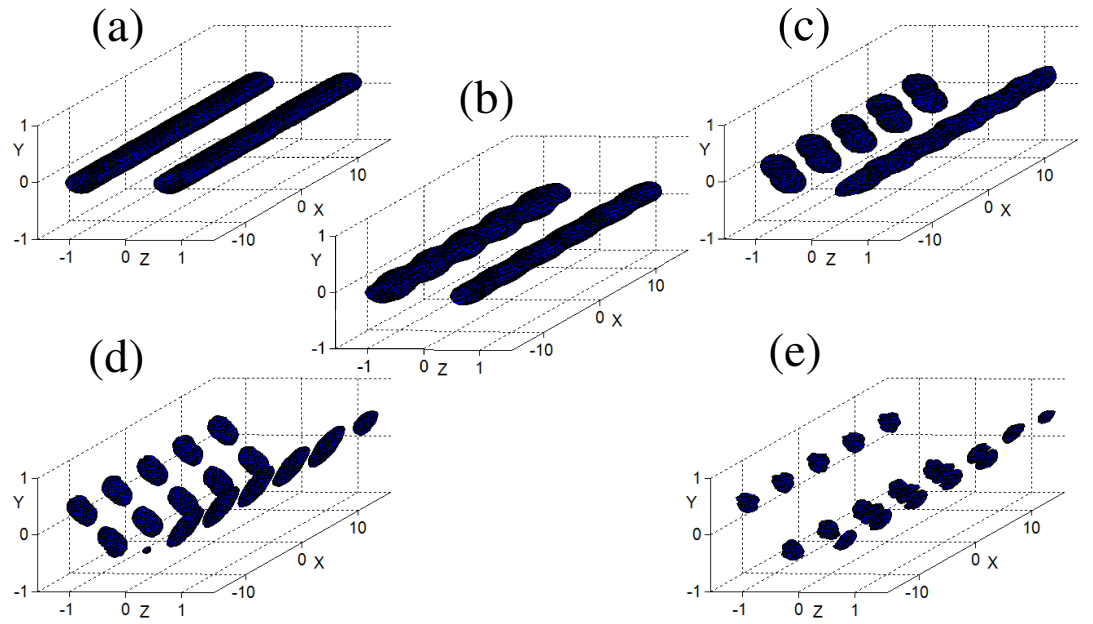

Figure 7. Vortex dynamics during transition as obtained analytically for the even transient growth perturbation. The secondary disturbance is assumed to have a constant growth rate and eigenfunction corresponding to $t_s = 20$. (a) $t = 0$,$Q/Q_{max} = 0.7$; (b) $t = 5$, $Q/Q_{max} = 0.7$; (c) $t = 10$, $Q/Q_{max} = 0.7$; (d) $t = 15$, $Q/Q_{max} = 0.7$; (e) $t = 20$, $Q/Q_{max} = 0.7$.

References

[1] Schmid, P. J. and Henningson, D. S., *"Stability and transition in shear flows"*, Springer-Verlag New York, 2001.

[2] Ellingsen, T. and Palm, E., "Stability of linear flow," *Phys. Fluids*, Vol. 18, 1975, pp. 487–488.

[3] Hultgren, L. S. and Gustavsson, L. H., "Algebraic growth of disturbances in a laminar boundary layer," *Phys. Fluids*, Vol. 24, 1981, pp. 1000.

[4] Ben-Dov, G., Levinski, V., and Cohen, J., "On the mechanism of optimal disturbances: The role of a pair of nearly parallel modes," *Phys. Fluids*, Vol. 15, 2003, pp. 1961–1972.

[5] Cohen, J., Philip, J., and Ben-Dov, G., "Aspects of linear and nonlinear instabilities leading to transition in pipe and channel flows," *Phil. Trans. R. Soc. A*, Vol. 367, 2009, pp. 509527.

[6] Zikanov, O. Y., "On the stability of pipe Poiseuille flow," *Phys. Fluids*, Vol. 8, 1996, pp. 2923–2932.

[7] Meseguer, A., "Streak breakdown instability in pipe Poiseuille flow," *Phys. Fluids*, Vol. 15, 2003, pp. 1203–1213.

[8] Butler, K. and Farrell, B., "Three-dimensional optimal perturbations in viscous shear flow," *Phys. Fluids A*, Vol. 4, 1992, pp. 1637–1650.

[9] Reddy, S., Schmid, P., Baggett, J., and Henningson, D., "On the stability of streamwise streaks and transition thresholds in plane channel flows," *J. Fluid Mech.*, Vol. 365, 1998, pp. 269–303.

[10] Gibson, J. F., "Channelflow: A spectral Navier-Stokes simulator in C++," Tech. rep., U. New Hampshire, 2012, `Channelflow.org`.

[11] Hunt, J., Wray, A., and Moin, P., "Eddies, stream, and convergence zones in turbulent flows," *Center for Turbulence Research Report CTR-S88*, 1988, pp. 193–208.